CATRINA (2025), 35(1):1-16

Biodiversity of Microfauna Dwelling Skin and Gills of *Clarias gariepinus* Burchell, 1822 from Polluted and Fragmented Habitats

Amer A. Noaman, Ahmed M. El-Naggar, Sayed A. El-Tantawy, Mohamed I. Mashaly*
Zoology Department, Faculty of Sciences, Mansoura University, Mansoura, Egypt

Received: July 8, 2024; Accepted: July 4, 2025

ABSTRACT

Aquatic ecosystems are increasingly threatened by anthropogenic pollution, which can profoundly impact host-parasite interactions and biodiversity. Understanding the relationships between environmental stressors and parasite communities is essential for effective monitoring and management of freshwater health. This study investigated the community structure and environmental determinants of ectoparasitic microfauna on the skin and gills of *Clarias gariepinus* across three Nile Delta ecosystems: the River Nile, Al-Amlak Drain, and a Quaternary Stream. Marked spatial variation in physicochemical parameters and heavy metal concentrations was observed, with Al-Amlak Drain exhibiting the highest pollution levels and lowest dissolved oxygen. Parasitic infestation was greatest at Al-Amlak Drain, while the Quaternary Stream displayed the highest species diversity. *Macrogyrodactylus* and *Gyrodactylus* species were more prevalent on the skin, and *Piscicola geometra* was restricted to polluted sites. Multivariate analyses revealed that the abundance and distribution of monogenean parasites were significantly influenced by specific water quality parameters and heavy metal profiles, with distinct ecological preferences observed between parasite species. These findings highlight the utility of monogenean parasites as sensitive bioindicators for assessing freshwater ecosystem health and the impacts of pollution.

Keywords: Aquatic ecosystems; Catfish; *Clarias gariepinus;* Ectoparasites; Fragmented Ecosystems; Microfauna; Water quality.

INTRODUCTION

The biodiversity of microfauna residing on the skin and gills of *Clarias gariepinus* (Burchell, 1822), a species of freshwater catfish, plays a critical role in the aquatic ecosystem, influencing both the health of the fish and the environment. In polluted and fragmented habitats, these microfaunal communities, which include various protozoans, copepods, and parasitic organisms, often experience significant alterations due to environmental stressors such as contamination, habitat destruction, and reduced water quality. Understanding the composition and diversity of these microfauna is essential for assessing the ecological impact of pollution on aquatic life, as these organisms serve as indicators of ecosystem health and can reflect the degree of habitat degradation.

Typically, fish gills are composed of arches, filaments, lamellae and rakers. The gill is one of the most vital organs in fish due to its physiological roles in ammonia nitrogen excretion, filter-feeding, respiration, and osmoregulation. The rakers provide fish with protection against debris. Gill filaments are feathery arrangements that are held by the curved gill arch. Gill lamellae increase surface respiratory area to optimize gas exchange process between water and blood. The gill lamellae extend from the gill filaments. Gas exchange primarily occurs at the gill lamellae, where the respiratory area is only one cell layer thick (Wilson and Laurent, 2002). The gill acts as a barrier to microbial, chemical, physical, and immunological threats. In addition to the aforementioned advantages, the gill apparatus of the catfish, *Clarias gariepinus*, is supplemented with an accessory breathing structure, namely the respiratory tree or dendritic organ (Karlina and Luthfi, 2018). Fish gills are preferred habitat for monogeneans, digeneans, crustaceans etc.

Host-parasite systems allow ecoparasitologists to explore fundamental aspects of ecology (Poulin and Morand, 2004; Poulin, 2007). Understanding how local parasite communities are structured and the nature of the interactions among cohabiting species in a particular habitat is one of the primary objectives of parasite ecology. Holmes and Price (1986) classified the communities of parasites into interactive (interactions among parasite species structure the community) and isolationist (interspecies interactions play a marginal role and the role of competition is minor). However, Salgado-Maldonado *et al.* (2020) suggested that interspecific competitive interactions could occur in species-poor communities, where aggregation determines the richness of local communities, and intraspecific aggregation permits species coexistence by reducing the overall intensity of interspecific competitive interactions.

Though parasites are widely hyped as signifying a great fraction of the total biodiversity around the globe, several questions remain around the degree of parasite diversity. In addition to their diversity in terms of abundance, monogeneans also differ in their morphology and ecology. Originally parasitic on the skin of early vertebrates, monogeneans have spread to

* *Corresponding author e-mail: dr.moh_mashaly@mans.edu.eg*

colonize the internal and external organs of a variety of aquatic vertebrates (mostly fish); they now exhibit a wide range of designs (Kearn, 1994; Whittington *et al.*, 2000). Egypt's drainage canals receive large volumes of wastewater from various sources of contamination (Salem *et al.*, 2021). Contaminants, such as various chemicals emitted from industrial processes, xenobiotics, and pesticides which may enhance oxidative stress by producing reactive oxygen species (Gabr *et al.*, 2020).

From an ecological perspective, in isolationist communities, the occurrence of a particular parasite species is independent of the presence of other cohabiting species (Rohde, 1979; Price, 1980). Conversely, in interactive, species-rich parasitic communities, both interspecific and intraspecific interactions among parasites are important forces that structure the community (Poulin and McDougall, 2022). In certain fish species, diverse communities of parasites have been identified, and interactions among these species have been documented (Agrawal *et al*., 2017). Therefore, the present study aims to characterize the community structure and species diversity of monogenean parasites affecting the gills and skin of the African sharptooth catfish, *Clarias gariepinus*, a native teleost of the River Nile system and a successful invader of artificial drains throughout the Nile Delta. This investigation will also assess the impact of water pollution and habitat fragmentation on these parasitic communities.

MATERIALS AND METHODS

Sampling sites and habitat descriptions

A total of 552 specimens of the African Sharptooth Catfish, *Clarias gariepinus* (Burchell, 1822), were collected using specialized fish nets from three distinct habitats in the Nile Delta (Fig. 1) between September 2021 and August 2022. The explored ecosystems included the River Nile (Damietta Branch) near Kafr El-Dabbosy (coordinates: 31°11'02.7"N, 31°30'11.-1"E), a Quaternary Stream that diverges from a tertiary tributary of the River Nile (coordinates: 30°58'46.5"N, 31°32'56.5"E), and a multisource polluted watercourse known as Al-Amlak Drain, located near Temay El Amdeed in Dakahlia Governorate (coordinates: 30°58'30.7"N, 31°31'22.6"E). Al-Amlak Drain serves as a common wastewater drainage channel traversing the eastern region of the Nile Delta, where it merges with Al-Nezam Drain, a typical agricultural drain, before flowing northward to discharge considerable volumes of polluted water into the southern area of Manzala Lake.

Physicochemical analysis of water samples

Water samples collected, from designated study sites using pre-cleaned polyethylene bottles were analyzed for physicochemical parameters following standard procedures outlined by the American Public Health aassociation (APHA, 2017, Al Shafei *et al.*, 2024). All measurements were conducted either *in situ* or immediately upon arrival at the laboratory to ensure accuracy. Temperature (°C) was measured *in situ* using a

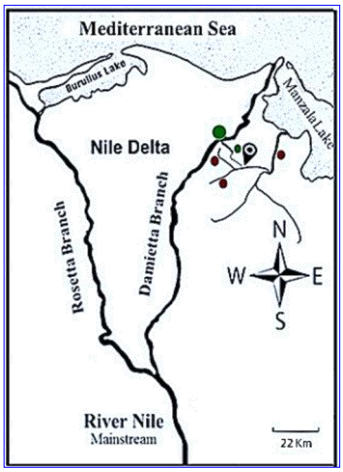

Figure (1): Hand-drawn map of the Nile Delta, Egypt, illustrating the River Nile habitat, including Kafr El-Dabbosy (represented by a large green solid circle), a Quaternary Stream (shown by a small green solid circle), and the Al-Amlak Drain (indicated by a red solid circle). The map includes a compass rose to indicate cardinal directions. The junction between the Quaternary Stream and the Al-Amlak Drain is clearly marked by .

calibrated digital thermometer. pH was determined in the field using a portable pH meter (Orion Research Model PTI20), which was calibrated prior to each measurement with standard buffer solutions (pH 4.0, 7.0, and 10.0). Total soluble salt (TSS) was measured using a CORNING (Cole-Parmer model Check 90) meter according to (APHA, 2017). Dissolved Oxygen (DO, mg/L): Measured in situ using a portable DO meter (Lutron YK-22DOA), using 0.1 N hydrochloric acid and methyl orange as an indicator, this parameter was measured by titration according to APHA (2017). Bicarbonate (HCO_3^-, mg/L) was determined by acid titration method using standard sulfuric acid (H_2SO_4) and methyl orange as an indicator.

Chloride (Cl^-, mg/L) was determined using the argentometric titration method with standard silver nitrate ($AgNO_3$) and potassium chromate as an indicator (APHA, 2017). Sulfate (SO_4^{2-}, mg/L) was also quantified gravimetrically by precipitation with a 5% barium chloride solution, according to APHA (2017). All measurements were conducted in triplicate to ensure precision and reproducibility. The results were compared across different study sites to evaluate spatial variations in water quality.

Heavy metal analysis in water samples

Collected water samples were filtered through Whatman filter paper, and the filtrates were stored at low temperatures until analysis. The concentrations of heavy metals were determined using a Buck Scientific Accusys 211 Atomic Absorption Spectrophotometer, following the method described by Allen *et al.* (1974). The detected heavy metal concentrations in the filtrate of the collected water samples were expressed in milligrams per liter (mg/L).

Sediment heavy metals analysis

A 0.5 g of the sediment was dried at 40 °C in an oven and then allowed to cool to room temperature. After that, samples of dry sediment were crushed, homogenized, and passed through a stainless steel sieve. Foll-

owing the procedures described in the PR NF ISO 14869-1 standard method, the dried, powdered, and sieved sediment fractions were promptly digested (AFNOR, 2001). Separately, 4 mL of bidistilled water was added to the dried sediment fractions to increase their humidity. The sediment blend was then carefully supplemented with 3 mL of perchloric acid ($HClO_4$) and 10 ml of hydrofluoric acid (HF). The mixture was then given twelve hours to settle. After that, the beaker was heated to 150°C for two hours. At that moment, the mixture was entirely evaporated. The digested components were filtered through 0.45 µm filter sheets and then diluted with 2% hydrochloric acid (HCl) to 100 mL.

Isolation and identification of monogenean parasites

Skin parasites were collected using sterile swabs followed by careful superficial scraping of the epidermal layer to ensure comprehensive sampling (Figure 2). For gill parasites, gill arches were dissected aseptically, and individual filaments were examined under a high-magnification stereomicroscope for metazoan parasites. Gill samples were preserved immediately in a 1:4000 formaldehyde/water fixative (Kritsky *et al*., 1986) to maintain parasite structural integrity. Microhabitat preferences of each parasite species were documented during examination, with particular attention to attachment sites on gill lamellae, filaments, and skin surfaces. Monogenean specimens were Isola-ted and identified based on morphological criteria: body dimensions, copulatory apparatus morphology, and sclerotized haptoral structures (hamuli, hooks, and connective bars). Comparative analysis of these features enabled species-level differentiation, consistent with established taxonomic keys for monogeneans.

Parasite collection and taxonomic identification

To collect monogenean worms from their attached locations on the skin and gills, a sharp needle was carefully inserted beneath the fixed haptor to detach the parasites and then were transferred to a glass slide, flattened under a coverslip, and examined for key morphological features of each monogenean species such as haptoral sclerites (hamuli, hooks, connective bars), copulatory complex structure, and vaginal tube architecture. Species identification was carried out using established taxonomic keys and authoritative references to ensure accurate classification of all ectoparasitic taxa collected. *Macrogyrodactylus clarii* was identified according to the original description by Gussev (1961), while *Macrogyrodactylus congolensis* was determined based on the diagnostic criteria outlined by Prudhoe (1957) and Yamaguti (1963). Identification of *Gyrodactylus rysavyi* followed the morphological features described by Ergens (1973). The leech *Piscicola geometra* was identified following the taxonomic guidelines of Lukin (1976).

Assessing biodiversity and community structure

To study community structure and species diversity in each ecosystem, the following ecological equations and indices were applied:

Simpson's Diversity Index (D)

Simpson's Diversity Index (D) measures diversity

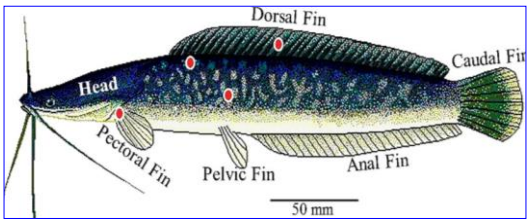

Figure (2): Skin map of the clariid host *C. gariepinus* showing the most favorable microhabitats (red solid circules) of *M. congolensis.* Scale bar = 50 mm.

by considering both the number of species present and the relative abundance of each species. As species richness and evenness increase, so does overall diversity. According to Dodge (2008), Simpson's Diversity Index (D) is calculated using the following equation:

$$D = \Sigma n_i(n_i\text{-}1) / N(N\text{-}1)$$

Where, n_i is the number of organisms that belong to species I; N, is the total number of organisms. The value of D ranges between 0 and 1. With this indicator, 1 represents infinite diversity and 0 represents no diversity.

Sorensen's similarity coefficient (Ss)

Sorensen's similarity coefficient (Ss) focuses on species that appear in both paired groups, rather than on mismatches in occurrences. This index was used to compare the species composition of the three distinct conditions of forest areas. According to Hammond and Pokorný (2020), Sorensen's similarity coefficient (Ss) is calculated as follows:

$$Ss = 2\ c / (S_1 + S_2)$$

Where, Ss is Sorensen's similarity coefficient; c, number of parasite species shared by both communities.

$$D=N(N-1)/\sum n(n-1)$$

Where, S_1 is the number of parasite species unique to first community; S_2 is the number of parasite species unique to second community.

Jaccard's similarity coefficient (SJ)

Jaccard's similarity coefficient (SJ), also known as the Jaccard index, is used to assess the similarity between two sets by quantifying the proportion of shared elements relative to the total number of unique elements in both sets. The coefficient ranges from 0% (no similarity) to 100% (complete similarity), with higher values indicating greater resemblance between the two populations. The similarity coefficient (SJ) is calculated using the following equation:

$$SJ = \frac{100c}{(a + b - c)}$$

Where, SJ is Jaccard's similarity coefficient; c is number of parasite species shared by both communities; a, is the number of parasite species unique to the first community and b is the number of parasite species unique to the second community.

Abundance and intensity

The mean abundance of parasites is calculated as the average number of individuals of a particular parasite species per host examined (including both infected and

uninfected hosts) following the equation:

$$A = \frac{\sum_{i}^{n} = 1\, P_i}{n_{\,examined}}$$

Where, *pi* is the number of parasites in the host (infected or uninfected hosts have *pi*=0) and n_{examine} is the total number of hosts examined.

However, for intensity, defined as a mean intensity which is the average number of individuals of a particular parasite species per infected host (only those hosts that are actually infected) following the equation:

$$A = \frac{\sum_{i}^{n} = 1\, P_i}{n_{\,infected}}$$

Where, pi is the number of parasites in the infected host. $n_{\text{ infected,}}$ is number of hosts infected with the parasite.

Statistical analyses

Multivariate statistical analyses using canonical correspondence analysis (CCA), as a direct gradient ordination technique, was performed using CANOCO software (ter Braak, 1986; 1988) to assess the relationships between monogenean species abundance and environmental variables. The CCA biplot displays sampling sites (points) across different seasons, while environmental variables, including physicochemical parameters and heavy metal concentrations, are represented as arrows.

RESULTS

Physicochemical analysis of water samples

The physicochemical parameters, temperature, pH, electrical conductivity (EC), and total dissolved solids (TDS), were measured across three aquatic environment sites: the River Nile (Damietta Branch), Al-Amlak Drain (a multisource pollution site), and the Quaternary Stream (a freshwater waterway) from September 2021 to August 2022 (Table 1). Results revealed that the River Nile exhibited the highest mean temperature (24.06 ± 5.48°C), with seasonal peaks, while the Al-Amlak Drain showed similar fluctuations but slightly higher maximum values. The Quaternary Stream maintained relatively stable and lower temperatures. pH levels remained alkaline at all sites, with the Al-Amlak Drain occasionally reaching higher values (peak 9.11), likely reflecting episodic pollution or organic matter decomposition.

EC and TDS were significantly higher in the Al-Amlak Drain (EC: 490.53 µS/cm; TDS: 346.99 mg/L), indicating elevated ionic and pollutant loads compared to the Nile and Quaternary Stream. Both EC and TDS peaked in the Al-Amlak Drain during late spring and early summer, coinciding with increased runoff and potential pollution events. These findings highlight the significant influence of multi-source pollution on water quality in the Al-Amlak Drain, in contrast to the relatively stable conditions observed in the River Nile and Quaternary Stream.

Table (2), presents the seasonal variation of several important water quality parameters: dissolved oxygen (DO_2), bicarbonate (HCO_3^-), chloride ions (Cl^-), and sulfate ions (SO_4^{2-}) which were measured across three selected aquatic environments during the period from September 2021 to August 2022 (Table 2).

Seasonal variations in dissolved oxygen (DO_2), bicarbonate (HCO_3^-), chloride (Cl^-), and sulfate (SO_4^{2-}) were recorded across the three sites in which the Nile exhibited the highest mean DO_2 (7.50 ± 1.76 mg/L), indicating stable oxygen conditions, while Al-Amlak Drain showed significantly lower DO_2 (6.56 ± 0.93 mg/L) with episodic depletion events. HCO_3^- concentrations were highest in the Nile (26.33 ± 8.08 mg/L), contrasting with Al-Amlak's reduced levels. Meanwhile, Cl^- and SO_4^{2-} were markedly elevated in Al-Amlak Drain (Cl^-: 300.96 ± 116.81 mg/L; SO_4^{2-}: 116.81 ± 46.97 mg/L), peaking at 479 mg/L and 472 mg/L respectively in May. These values exceeded those in the Nile (Cl^-: 136.47 mg/L; SO_4^{2-}: moderate) and Quaternary Stream, confirming pollution-derived ionic loading. The Quaternary Stream displayed intermediate Cl^-/SO_4^{2-} levels with seasonal fluctuations, while the Nile maintained consistency.

In general**,** the data indicate that the Al-Amlak Drain experiences elevated concentrations of chloride and sulfate ions, reflecting significant pollution inputs, which may adversely affect aquatic biota and water quality. The lower dissolved oxygen levels further suggest potential hypoxic stress conditions, likely due to organic pollution and microbial respiration. Conversely, the Nile and Quaternary Stream generally maintain better water quality parameters, although seasonal variations occur. These findings underscore the impact of pollution sources on the chemical dynamics of the studied aquatic systems, highlighting the need for targeted environmental management strategies.

Heavy analysis of water samples

The heavy metal concentrations varied significantly across sites and seasons (Table 3). River Nile site showed elevated aluminum and copper, indicative of anthropogenic influence. The Quaternary Stream consistently showed the highest mean concentrations of aluminum (19.74 ppm) and barium (0.92 ppm), with pronounced peaks during winter and spring. Zinc was notably higher at Al-Amlak Drain, especially in spring, likely reflecting industrial or agricultural inputs. Iron was recorded at the highest levels in winter among all sites, with the Al-Amlak Drain and the Quaternary Stream exhibiting the highest mean levels of (about 7.7 mg/L). Seasonal fluctuations in several metals, including lead and cadmium, highlight dynamic pollution sources. These spatial and temporal variations emphasize the need for continuous monitoring to inform effective management of heavy metal pollution in the Nile Delta.

Community structure of ectoparasitic microfauna on *Clarias gariepinus*

Out of 552 *Clarias gariepinus* catfish collected from the three investigated localities, a total of 8,164 worms were identified, with a number of 3,900 from the skin

Table (1): Physiochemical characterization of water across three studied sites: River Nile (Damietta Branch), Al-Amlak Drain (multisource pollution) and Quaternary Stream (freshwater waterway).

Month	Studied sites											
	River Nile (Damietta Branch)				Al-Amlak Drain (multisource pollution)				Quaternary Stream (freshwater waterway)			
	T (°C)	pH	EC (dS/m)	TDS (ppm)	T (oC)	pH	EC (dS/m)	TDS (ppm)	T (°C)	pH	EC (dS/m)	TDS (ppm)
September (2021)	28.90	7.88	0.32	202.88	29.60	8.19	0.83	530.56	29.70	8.15	0.76	487.04
October	28.20	8.00	0.32	199.04	26.90	8.33	0.75	474.88	26.50	7.94	0.35	278.40
November	25.00	8.46	0.31	195.20	22.50	8.46	0.66	419.20	22.50	8.40	0.30	278.40
December	16.40	8.51	0.36	227.20	16.90	8.49	0.85	540.80	16.00	8.38	0.39	193.30
January	15.35	8.62	0.30	192.00	14.60	8.69	0.74	476.16	16.10	8.49	0.44	248.32
February	16.40	8.55	0.30	192.32	16.70	8.51	0.80	512.00	16.30	8.55	0.43	272.64
March	19.50	8.48	0.30	192.64	19.90	8.46	0.79	506.90	18.40	8.40	0.38	240.60
April	24.20	8.42	0.53	335.64	23.90	8.48	0.77	490.53	24.60	8.40	0.54	342.51
May	25.20	9.11	0.29	187.52	26.00	8.60	0.89	572.16	25.60	8.72	0.84	535.68
June	31.30	9.00	0.32	201.60	29.90	8.64	0.81	520.32	34.30	8.66	0.86	380.80
July	29.20	8.70	0.30	193.90	32.50	8.69	0.49	315.50	32.30	8.64	0.60	355.20
August (2022)	29.10	7.66	0.31	199.68	37.80	8.25	0.82	527.36	32.50	8.05	0.56	551.00
Mean	24.06	8.45	0.33	209.97	24.77	8.48	0.77	490.53	24.57	8.40	0.54	346.99
±SD	5.48	0.41	0.06	39.11	6.74	0.16	0.10	64.51	6.48	0.23	0.18	114.63

Table (2): Water quality parameters at the studied sites: water across three studied sites: River Nile (Damietta Branch), Al-Amlak Drain (multisource pollution) and Quaternary Stream (freshwater waterway) during September 2021 to August 2022.

Month	Studied sites											
	River Nile (Damietta Branch)				**Al-Amlak Drain** (multisource pollution)				**Quaternary Stream** (freshwater waterway)			
	DO_2 (ppm)	**HCO_3^- (mgL^{-1})**	**Cl^- (mgL^{-1})**	**SO_4^{2-} (mgL^{-1})**	**DO_2 (ppm)**	**HCO_3^- (mgL^{-1})**	**Cl^- (mgL^{-1})**	**SO_4^{2-} (mgL^{-1})**	**DO_2 (ppm)**	**HCO_3^- (mgL^{-1})**	**Cl^- (mgL^{-1})**	**SO_4^{2-} (mgL^{-1})**
September (2021)	6.50	27.08	132.54	45.84	7.40	105.42	302.48	112.66	7.80	39.17	300.67	42.08
October	7.50	33.63	125.03	36.71	5.00	79.41	255.19	134.83	7.90	88.55	143.39	97.82
November	5.80	25.03	121.81	52.21	7.00	53.39	207.90	157.00	7.00	12.66	110.90	69.74
December	8.80	16.42	111.07	67.71	5.50	73.22	281.80	185.80	9.50	22.41	175.40	80.64
January	11.30	18.44	131.40	77.32	5.80	66.77	202.90	136.13	9.50	43.38	151.95	52.99
February	10.50	33.37	113.03	45.60	5.70	69.88	284.26	157.86	9.90	47.04	144.40	66.75
March	7.40	32.41	115.50	44.41	6.30	76.44	270.50	159.90	8.00	41.22	185.85	55.01
April	6.30	31.45	117.97	43.22	6.80	64.87	300.96	116.81	7.30	37.92	250.04	56.96
May	7.70	42.68	147.35	72.93	8.40	34.88	479.06	58.22	6.90	25.41	472.00	37.75
June	6.70	17.08	146.56	23.88	6.40	31.95	441.82	46.55	6.30	22.96	329.93	27.91
July	5.80	18.95	157.53	25.12	6.80	21.92	262.40	31.20	5.90	26.64	484.90	39.45
August (2022)	5.70	19.44	217.88	27.11	7.60	100.34	322.25	104.77	6.70	47.71	251.07	56.42
Mean	7.50	26.33	136.47	46.84	6.56	64.87	300.96	116.81	7.73	37.92	250.04	56.96
±SD	1.76	8.08	28.36	17.29	0.93	24.67	79.29	46.97	1.26	18.64	120.62	18.82

Table (3): Seasonal fluctuations of selected heavy metals in subsurface water from the River Nile (Damietta Branch), Al-Amlak Drain and Quaternary Stream.

Studied sites†	Season	Studied sites													
		Measured parameters (PPM)													
		Al	Ag	Ba	Cd	Co	Cu	Fe	Ga	Mn	Ni	Pb	Sr	Zn	Bi
1		7.350	1.460	1.044	0.259	0.180	0.630	7.392	1.242	0.233	0.284	0.944	0.648	4.646	0.120
2	**Summer**	3.757	1.619	1.049	0.258	0.100	0.844	7.823	ND	0.285	0.210	0.998	0.666	5.618	0.330
3		11.633	1.612	1.040	0.262	0.187	0.754	7.700	0.146	0.256	0.090	1.021	0.640	4.663	0.895
1		15.766	1.073	0.901	0.242	0.107	1.500	5.479	0.234	0.081	0.433	0.295	0.583	4.280	0.265
2	**Autumn**	0.903	2.142	0.816	0.210	ND	0.633	4.496	0.195	0.209	ND	1.053	0.614	4.417	1.472
3		5.193	1.446	0.961	0.238	0.218	0.610	4.493	0.215	0.063	0.434	0.914	0.511	4.752	0.226
1		2.977	1.088	2.062	0.273	0.128	ND	11.762	ND	0.492	0.124	1.696	0.831	4.727	0.115
2	**Winter**	7.963	1.404	0.846	0.321	0.194	1.180	9.548	0.216	0.273	0.361	1.203	0.757	4.982	0.612
3		35.996	1.112	0.818	0.316	0.191	0.198	10.700	0.126	0.313	ND	0.743	0.730	4.405	0.074
1		2.250	1.955	0.903	0.215	0.239	0.491	5.268	1.374	0.200	0.068	0.702	0.511	4.956	0.600
2	**Spring**	1.893	1.498	1.024	0.210	0.131	1.153	5.352	0.354	0.263	0.393	0.755	0.695	11.435	0.249
3		26.147	2.135	0.873	0.258	0.151	1.410	7.632	ND	0.244	0.288	0.836	0.526	4.402	1.386
1		7.086	1.394	1.228	0.247	0.164	0.874	7.475	0.950	0.252	0.227	0.909	0.643	4.652	0.275
2	**Mean**	3.629	1.666	0.934	0.250	0.142	0.953	6.805	0.255	0.258	0.321	1.002	0.683	6.613	0.666
3		19.742	1.576	0.923	0.269	0.187	0.743	7.631	0.162	0.219	0.271	0.879	0.602	4.556	0.645
1		6.210	0.415	0.560	0.025	0.059	0.547	3.013	0.624	0.173	0.165	0.589	0.137	0.281	0.228
2	**SD**	3.122	0.329	0.120	0.053	0.048	0.262	2.310	0.086	0.034	0.098	0.186	0.060	3.252	0.560
3		13.936	0.427	0.098	0.033	0.028	0.503	2.534	0.047	0.108	0.173	0.118	0.103	0.179	0.609

† Studied sites: 1, River Nile (Damietta Branch); 2, Al-Amlak Drain; and 3, Quaternary Stream. ND, not detected.

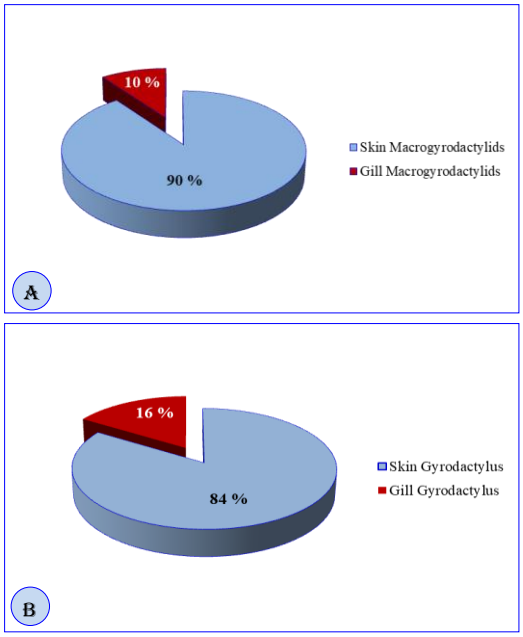

Figure (3): illustrates the distribution ratios of two parasite species, *Macrogyrodactylus* sp. (A) and *Gyrodactylus* sp. (B), on different parts of the studied *Clarias gariepinus* fish, as a comparison of skin verses gills.

surface and fins (including *Macrogyrodactylus*, *Gyrodactylus*, and *Piscicola geometra*) and 4,264 from the gills (which comprised 2,387 *Quadriacanthus* worms, 214 *Macrogyrodactylus* worms, 358 *Gyrodactylus* worms, and 1,305 digenean cysts). Parasitic load varied among habitats, with 40.4% in Al-Amlak Drain, 31.0% in the River Nile, and 28.6% in the Quaternary Stream.

Regarding the skin dwellers, a total of 3,900 ectoparasitic worms were encountered, including 3,883 monogenean worms (99.56%) and 17 hirudinean leeches, *Piscicola geometra* (0.43%). The monogenean assemblage on the skin was comprised of 1,935 *M. congolensis* worms (49.62%) and 1,948 *Gyrodactylus rysavyi* worms (49.95%). For the genus *Macrogyrodactylus*, the skin-dwelling *M. congolensis* displayed a sharing ratio of 90%, while thegill-resident *M. clarii* had a sharing ratio of 10% (Fig. 3A). Similarly, for the genus *Gyrodactylus*, the skin-dwelling *G. rysavyi* recorded a sharing ratio of 84%, while the gill-resident *G. clarii* had a sharing ratio of 16% (Fig. 3B).

Similarity and diversity of ectoparasitic communities on *Clarias gariepinus*

The figure (4A) presents the percentage distribution of parasites between the skin and gill of the catfish, *Gyrodactylus rysavyi*, at the three studied sites: The River Nile, Amlak, and Stream. The distribution patterns reveal notable site-specific differences:

At the River Nile site, the majority of parasites were found on the gill, with a smaller proportion on the skin (32.5% and 51.4, respectively). This result reflects that the gill harbored about 55% of the total parasite load. In contrast, at the Amlak site, the distribution was more heavily skewed towards the gills, with 51.6 % of parasites located on the gills and only 30.4% on the skin. For the Stream site, the distribution was nearly even, with the skin hosting almost 16% and the gills 18.2% of the parasites. These results indicate distinguished site-specific differences in parasite localization which recorded different physiochemical characterization and heavy metal pollutants. In general, the stream site displays the lowest overall parasite prevalence, with a slight predominance on the gills. For the River Nile site, shows a relatively higher distribution on gill verses skin, whereas Amlak is characterized by a much higher prevalence of parasites on the gills (Figure 4A).

The percentage distribution of *Macrogyrodactylus congolensis* detected on the skin of catfish collected from same studied sites recorded that the highest prevalence was observed at the Amlak Drain site, accounting for 35.9% of the total skin-infesting para-sites. This was followed by the River Nile, with 33.9%, and the Stream, with the lowest prevalence at 30.2% (Figure 4B). These results indicate that catfish inhabiting the Amlak Drain are more heavily infested with *M. congolensis* on their skin compared to those from the River Nile and Stream. The elevated prevalence at Al-Amlak Drain may be attributed to the higher pollution levels, increased organic matter, or degraded water quality, which can create favorable conditions for para-site proliferation (Table 1 and 2). In contrast, the lower prevalence in the Stream suggests comparatively better environmental conditions or lower host density, reducing opportunities for parasite transmission.

Based on the distribution ratios of *Macrogyrodactylus clarii* on catfish gills across the three studied localities (Figure 4), showed that the prevalence in the River Nile recorded the highest proportion of *Macrogyrodactylus clarii* (45.3%). However, the Al-Amlak

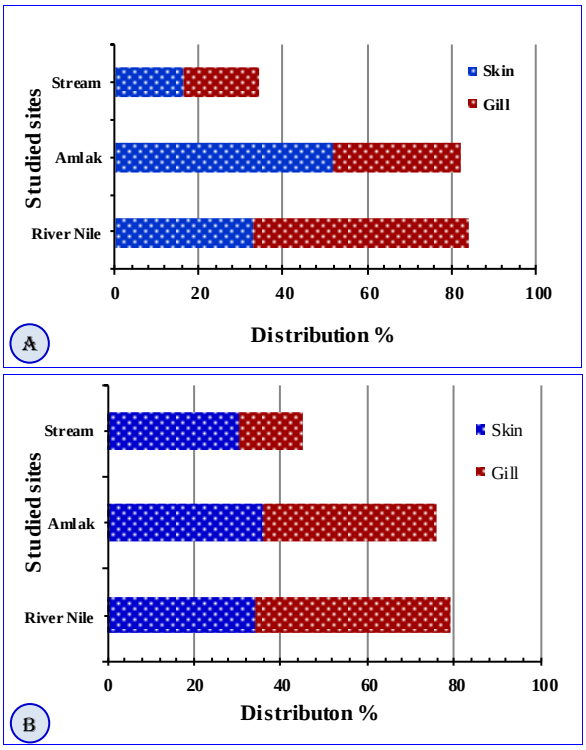

Figure (4): Distrubtion percentage of different epiparasite on skin and gill of catfish collected from different locations: The River Nile, Amlak, and Stream. A, *Gyrodactylus rysavyi*; B, *Macrogyrodactylus congolensis.*

Drain exhibited a substantial prevalence (39.7%), suggesting that despite elevated pollution levels, it remains a suitable environment for *M. clarii*. Conversely, the Quaternary Stream recorded the lowest prevalence (15%), which may reflect suboptimal physicochemical or ecological conditions limiting the parasite's establishment and transmission potential. These spatial differences underscore the influence of habitat quality and environmental factors on the epidemiology of monogenean parasites in freshwater systems (Figure 4).

For comparison, similarity indices, including Sørensen and Jaccard coefficients, demonstrated complete similarity of ectoparasitic communities between the River Nile and the Quaternary Stream habitat (SS and JS = 1.00). Additionally, high levels of similarity were observed between the River Nile and Al-Amlak Drain (SS and JS = 0.94 and 0.89, respectively), as well as between the Quaternary Stream and Al-Amlak Drain (SS and JS = 0.94 and 0.89, respectively). The Simpson Index indicated a high diversity of ectoparasitic communities on *C. gariepinus* across different habitats. The Simpson's Reciprocal Index values were 5.18 for the River Nile, 4.88 for Al-Amlak Drain, and 5.35 for the Quaternary Stream, suggesting considerable heterogeneity within these communities.

Correlation between water physicochemical variables and prevalence of monogenean parasites

Significant positive correlations were observed between several physicochemical parameters, namely sulfates, calcium, bicarbonates, chlorides, temperature, sodium, and electrical conductivity, and the first two axes representing the prevalence of monogenean parasites (*Macrogyrodactylus and Gyrodactylus* spp.) infecting *C. gariepinus*. Both parasite genera clustered near the center of the ordination axes, suggesting that these physicochemical factors exert similar influences on their prevalence (Fig. 5A). In terms of species distribution, *M. clarii* is positioned toward the lower left quadrant of the ordination diagram, indicating a stronger association with specific environmental conditions characterized by elevated pH and total dissolved solids (TDS). *G. rysavyi* appears to be located in close proximity to *M. clarii*, suggesting potential overlap in ecological niches or similar habitat preferences.

Correlation between heavy metal content and prevalence of monogenean parasites

The CCA biplot presents the relationship between heavy metal variables and the distribution of two monogenean parasite species (*M. clarii* and *G. rysavyi*) infecting *C. gariepinus*. The environmental variables (heavy metals) are represented as vectors, where the direction and length of each arrow indicate the strength and orientation of the correlation with the canonical axes. Both *G. rysavyi* and *M. clarii* are positioned in the lower quadrants of the plot, suggesting that their prevalence is influenced by specific heavy metals. *M. clarii* shows a closer association with Aluminum (AL), Mn, and a moderate correlation with cobalt indicating a

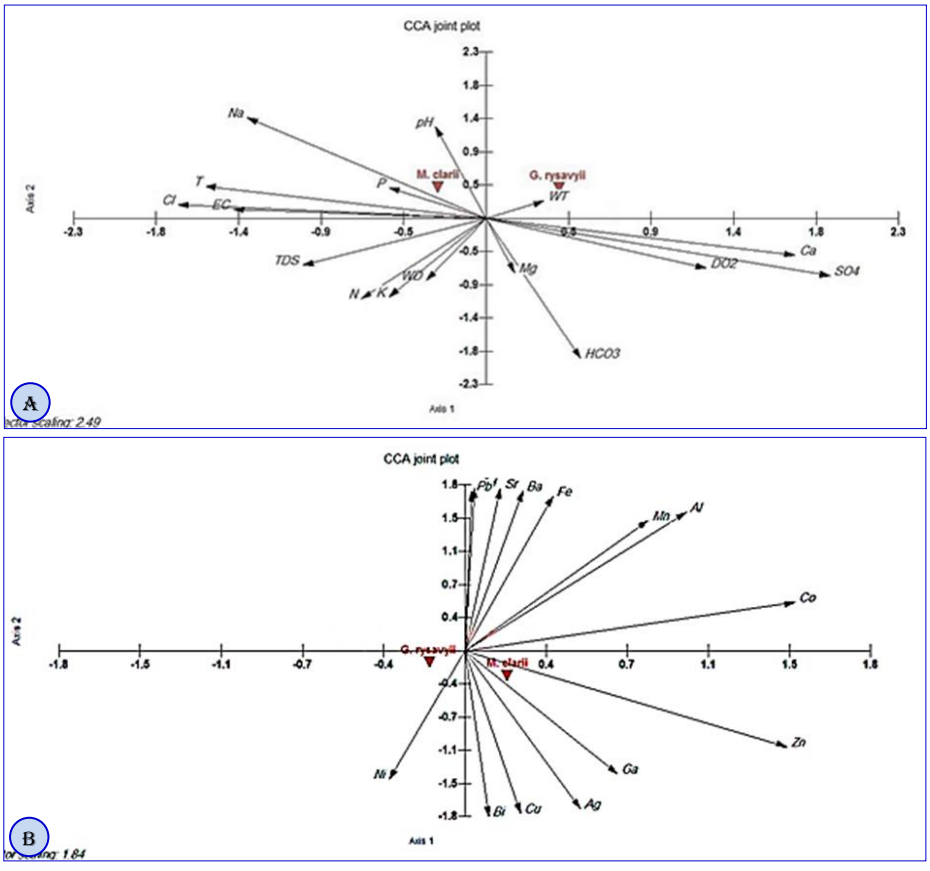

Figure (5): Canonical corresponding analysis (CCA) ordination diagram of the prevalence values of the different ectoparasites (*Macrogyrodactylys and Gyrodactylus spp*., indicated by red arrows) infected catfish, *C. gariepinus* according to the gradient of the parameter measured. A, Physiochemical characterization; B, heavy metals variables during the four seasons in the study sites.

potential preference for or tolerance to environments with elevated concentrations of these metals. In contrast, *G. rysavyi*, located slightly left of the origin, demonstrates a modest association with strontium (Sr), barium (Ba), and iron (Fe).

Conversely, metals such as Bi, Cu, Ga, Ag, Zn, and Ni extend in directions opposite to both parasite species, implying a possible negative correlation with their occurrence. The separation of routes such as Co, Zn, and Ga suggests these metals exert distinct environmental pressures or influences on parasite distribution (Figure 5B). The clustering of routes with similar orientations like Pb, Sr, Ba and Fe also indicates possible covariation among these metals, potentially arising from similar anthropogenic sources.

Correlation between water physicochemical and intensity of monogenean parasites

The CCA biplot illustrates the associations between various physicochemical water parameters and the distribution intensity of monogenean parasites (*M. clarii* and *G. rysavyi*) infecting *C. gariepinus*. Environmental variables are represented as arrows, with direction and length indicating the gradient and strength of correlation with the first two canonical axes. Both *M. clarii* and *G. rysavyi* are clustered near the origin of the plot, indicating a moderate, non-exclusive association with several physicochemical variables. Their existence in this position suggests that multiple overlapping environmental factors influence their intensity rather than strong dependence on a single dominant variable. Remarkably, parameters such as Ca, SO_4^{2-}, Mg, HCO_3^-, K, NO_3^-, TDS, and temperature (T^oC) point toward the upper right quadrant of the plot, suggesting a positive correlation with Axis 1 and possibly a role in shaping the ecological niches of the parasite species. On the other hand, pH, Na, EC, and Cl^- routes extend toward the left and lower quadrants, indicating a negative correlation along Axis 1 and a contrasting environmental influence (Figure 7A). Meanwhile, the position of DO_2 in proximity to the parasite species suggests that DO_2 levels may have a mild positive influence on their intensity, although this relationship is not strongly directional. In general, the figure (6 A) reflects the complexity of interactions between environmental conditions and parasite prevalence, highlighting the need to consider multiple water quality variables when assessing ecological risk or parasite load in freshwater systems.

Correlation between water heavy metal content and intensity of monogenean parasites

CCA biplot analysis reveals (6B) distinct relationships between heavy metal concentrations and the intensity of two monogenean parasite species, *M. clarii* and *G. rysavyi*, infecting *C. gariepinus*. *M. clarii* is positively correlated with metals such as iron (Fe) and barium (Ba), suggesting that increased concentration of these elements may favor its prevalence and intensity. Conversely, *G. rysavyi* appears to be influenced by str-

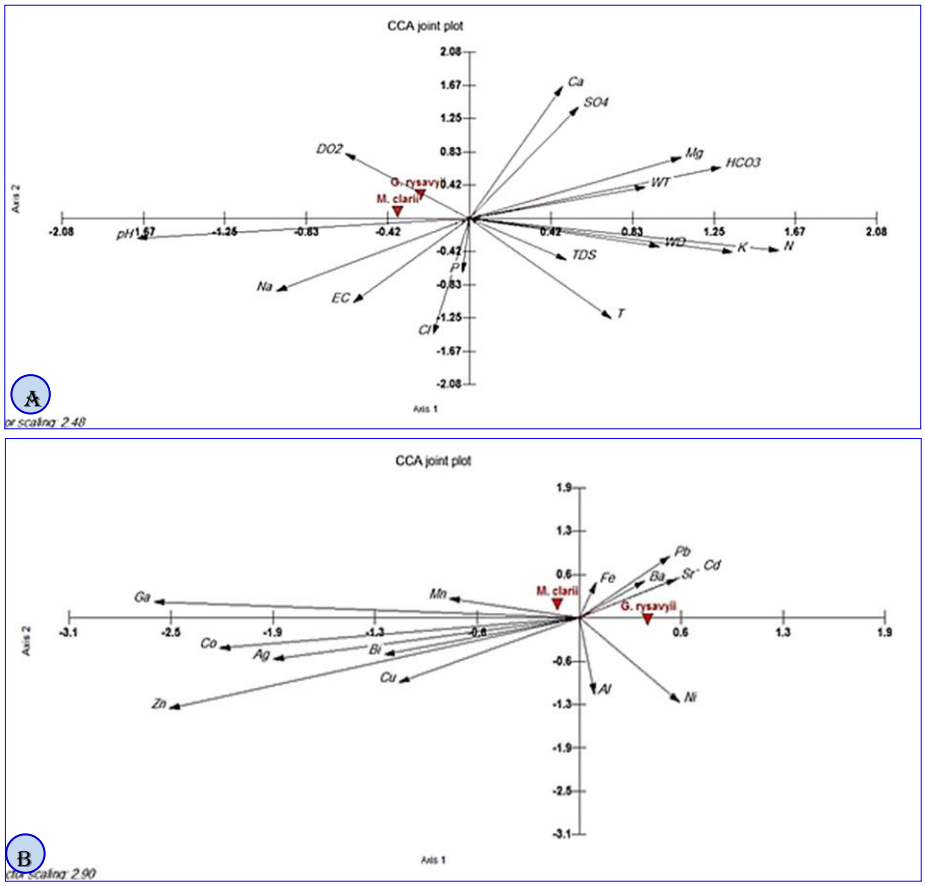

Figure (6): Canonical corresponding analysis (CCA) ordination diagram of the mean of intensity values of the different ectoparasites (*Macrogyrodactylys* and *Gyrodactylus* spp., indicated by red arrows) infected catfish, *C. gariepinus* according to the gradient of the parameter measured. A, Physiochemical characterization; B, heavy metals variables during the four seasons in the study sites.

ontium (Sr) and lead (Pb), indicating that its distribution is shaped by different environmental conditions (Figure 6B). Additionally, measured heavy metals like copper (Cu), zinc (Zn), and cadmium (Cd) show a negative correlation with both parasite species, implying that elevated levels of these metals could hinder their survival and reproduction. The separation of routes highlights the unique environmental pressures exerted by different heavy metals, emphasizing the need for further investigation into how anthropogenic activities may impact parasitic dynamics in aquatic ecosystems. Understanding these relationships is critical for developing effective management strategies to mitigate parasitic infections in fish populations.

Correlation between water physicochemical and abundance of monogenean parasites

The CCA biplot illustrates the relationships between various physicochemical water parameters and the distribution patterns of two monogenean parasites, *M. clarii* and *G. rysavyi*, infecting *C. gariepinus.* The ordination reveals distinct ecological preferences for the the two parasite species based on environmental gradients. *G. rysavyi* is positioned in the upper right quadrant of the biplot, indicating a strong positive association with DO_2, Ca^{2+}, Mg^{+1}, SO_4^{2-}, and HCO_3^-. This suggests that the presence of *G. rysavyi* is favored in well-oxygenated environments with higher hardness and buffering capacity, possibly reflecting cleaner or more stable aquatic conditions. In contrast, *M. clarii* is situated toward the left side of the plot, showing closer association with parameters such as EC, Na^+, pH, T, P^3, TDS, and Cl^-. These variables are typically indicative of increased ionic content or anthropogenic influence, suggesting that *M. clarii* may be more tolerant of eutrophic or disturbed conditions. The opposing distribution of the two parasite species along the first canonical axis (Axis 1) suggests divergent ecological niches, with *G. rysavyi* being more associated with cleaner water conditions and *M. clarii* linked to environments with higher salinity and nutrient loads. This differentiation highlights the influence of specific water quality parameters on parasite prevalence and community structure in fresh-water systems (Figure 7A).

Correlation between heavy metals and abundance of monogenean parasites

Zinc and cobalt concentrations exhibited strong and statistically significant correlations with the first and second ordination axes representing the abundance of monogenean parasites (*Macrogyrodactylus* and *Gyrodactylus* spp.) infecting *C. gariepinus* (Figure 7B). Both parasite genera were positioned near the center of the ordination plot, indicating that these heavy metals similarly influence their abundance.

For *M. clarinii* is located on the positive side of axis 1, showing a strong positive association with several metals including Zn, Ag, Cu, Bi, Al, Ga, Co, and Mn. The direction and magnitude of these routes suggest that higher concentrations of these elements may be positively correlated with increased abundance of *M. clarinii*, possibly indicating a tolerance to or preference

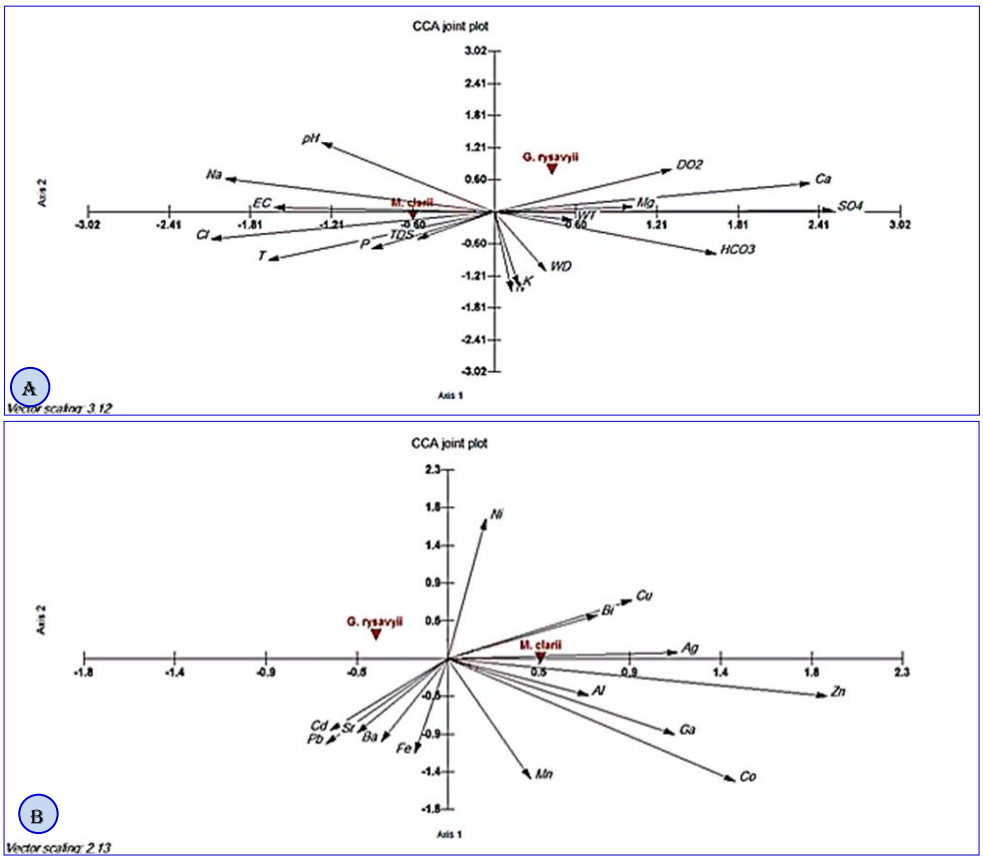

Figure (7): Canonical corresponding analysis (CCA) ordination diagram of the mean of intensity values of the different ectoparasites (*Macrogyrodactylys* and *Gyrodactylus* spp., indicated by red arrows) infected catfish, *C. gariepinus* according to the gradient of the parameter measured. A, Physiochemical characterization; B, heavy metals variables during the four seasons in the study sites.

for hosts exposed to such metals.

In contrast, *G. rysavyii* is positioned on the negative side of Axis 1 and is more closely associated with Pb, Cd, Sr, Ba, and Fe. This implies a different pattern of correlation, where the abundance of *G. rysavyii* increases in environments or host tissues with elevated levels of these particular metals. The divergence in metal associations between the two parasites highlights species-specific responses to environmental contamination. In general, the CCA plot supports the hypothesis that the abundance of parasitic species is influenced by the profile of heavy metal contamination. These findings underscore the potential utility of parasite populations as bioindicators for assessing ecological impacts of heavy metal pollution in freshwater systems (Figure 7A-B).

DISCUSSION

The results of this study provide valuable insights microfauna inhabiting the skin and gills of *Clarias gariepinus* across different aquatic environments. The prevalence of parasitic infestation varied significantly among habitats, with the highest infestation rate observed in the Al-Amlak Drain (40.4%), followed by the River Nile (31.0%) and the Quaternary Stream (28.6%). This spatial variation aligns with previous findings that environmental stressors, such as pollution and habitat degradation, can substantially influence the abundance and diversity of parasite communities (El-Emam *et al*., 2024; Salgado-Maldonado *et al*., 2020) and Sue *et al.*, 2022).

The predominance of ectoparasitic worms on the skin of *C. gariepinus*, with monogeneans constituting over 99% of the total parasites identified, underscores the ecological importance of the skin as a primary microhabitat for these parasites. The dominance of *M. congolensis* and *G. rysavyi* aligns with previous findings that monogeneans preferentially colonize the skin due to its relatively stable conditions, which facilitate attachment and feeding compared to the more dynamic gill environment (El-Shaer and Sallam, 2023; Kearn, 1994). The marked microhabitat specificity, reflected in the high sharing ratios of skin-associated species (*M. congolensis* 90%, *G. rysavyi* 84%) relative to their gill-resident counterparts, suggests that these parasites have adapted to exploit the skin niche effectively. This preference likely confers advantages such as enhanced feeding efficiency and reduced exposure to host immune responses and predation pressures (Chalkowski *et al*., 2018). Moreover, these microhabitat-driven distribution patterns contribute significantly to the structuring of parasite communities on *C. gariepinus*. Importantly, environmental factors such as pollution may modulate these patterns by altering host physiology and habitat quality, thereby influencing parasite abundance and diversity, as supported by previous studies (Salgado-Maldonado *et al*., 2020; Sue *et al*., 2022). These findings highlight the complex interplay between host microhabitats and environmental stressors in shaping ectoparasitic assemblages.

The observed site-specific differences in the distribution of *G. rysavyi* between the skin and gills of *C. gariepinus* reflect the complex interplay between environmental conditions and parasite ecology. At the River Nile site, parasites were more evenly distributed, with a slight predominance on the gills (55% of total parasite load), whereas the Al-Amlak Drain exhibited a stronger slope towards gill infestation (51.6%), and the Stream site showed a nearly balanced but overall lower parasite prevalence. These patterns align with previous studies demonstrating that parasite localization on fish hosts can be influenced by habitat-specific factors such as water quality, pollution, and host physiology (Salgado-Maldonado *et al.*, 2020; El-Shaer and Sallam, 2023).

The higher gill infestation at the Al-Amlak Drain corresponds with its documented elevated pollution levels, including increased heavy metals and organic pollutants, which may impair host immune defenses and promote parasite proliferation (Abdel-Satar *et al.*, 2017; Sue *et al.*, 2022). Polluted environments often alter host susceptibility and parasite transmission dynamics by stressing fish and modifying microhabitat conditions on the host surface, favoring parasites that exploit gill tissues, which provide rich oxygen and nutrient supplies (Kearn, 1994). Conversely, the Stream site, with relatively better physicochemical parameters and lower pollution, exhibited reduced parasite loads, consistent with findings that improved water quality correlates with lower parasite prevalence and intensity (Fanack Water Quality in Egypt, 2023).

Regarding *M. congolensis*, the highest skin infestation prevalence at the Al-Amlak Drain (35.9%) further supports the view that degraded water quality enhances parasite success on the skin microhabitat. This is in agreement with El-Shaer and Sallam (2023), who reported increased monogenean infestations in polluted waters due to favorable conditions for parasite reproduction and transmission. The relatively lower prevalence at the Stream site (30.2%) likely reflects reduced host density or environmental conditions less conducive to parasite survival, as also suggested by Salgado-Maldonado *et al*. (2020).

In general, these findings highlight the significant influence of environmental stressors, particularly pollution, on the spatial distribution and prevalence of ectoparasites on *C. gariepinus*. The differential parasite localization between skin and gills across sites underscores the importance of microhabitat-specific ecological factors and host-parasite interactions shaped by habitat quality. These results emphasize the need for integrated environmental management to mitigate pollution impacts and preserve aquatic ecosystem health.

Significant positive correlations between physicochemical parameters, such as sulfates, calcium, bicarbonates, chlorides, temperature, sodium, and electrical conductivity, and the prevalence of *Macrogyrodactylus* and *Gyrodactylus* spp. indicate that water chemistry strongly influences monogenean parasite distribution on *C. gariepinus*. The close clustering of

these parasites suggests similar ecological responses to environmental factors. *M. clarii*'s association with elevated pH and total dissolved solids aligns with previous findings that certain monogeneans thrive in alkaline, mineral-rich waters (El-Shaer and Sallam, 2023). The overlap with *G. rysavyi* supports shared habitat preferences. These recorded data are in agreement with earlier observations of higher parasite loads in polluted sites, highlighting how altered water quality can enhance parasite prevalence by affecting host susceptibility and parasite trans-mission (Salgado-Maldonado *et al*., 2020; Sue *et al*., 2022). Integrating physicochemical data with parasitological studies is thus crucial for understanding and managing parasite dynamics in freshwater ecosystems.

For the correlation between monogens parasities and heavy metal polluted the water sources at which the study done, the CCA results indicate that *M. clarii* is positively associated with aluminum, manganese, and cobalt, suggesting tolerance to these metals, while *G. rysavyi* correlates moderately with strontium, barium, and iron. Metals such as copper, zinc, and nickel showed negative correlations with both parasites, likely due to their toxic effects on parasite survival, consistent with previous studies (Abdel-Satar *et al*., 2017; Kumari *et al*., 2019; Salgado-Maldonado *et al*., 2020). The clustering of lead, strontium, barium, and iron suggests common pollution sources influencing parasite distribution (Cambridge Core, 2003). These findings highlight species-specific responses of monogeneans to heavy metal pollution, emphasizing the complex impact of contaminants on parasite ecology.

The calculated intensity and abundance of the studied epiparasites, the CCA analysis reveals contrasting ecological preferences between *G. rysavyi* and *M. clarii* in relation to water physicochemical variables. *G. rysavyi* shows a strong positive association with dissolved oxygen, calcium, magnesium, sulfate, and bicarbonate, parameters indicative of well-oxygenated, stable, and less polluted waters. This aligns with previous studies reporting that *Gyrodactylus* species tend to thrive in cleaner freshwater environments with good water quality (El-Shaer and Sallam, 2023; Salgado-Maldonado *et al*., 2020). Conversely, *M. clarii* correlates with higher electrical conductivity, sodium, pH, temperature, phosphate, total dissolved solids, and chloride, suggesting a tolerance for eutrophic or anthropogenically impacted habitats. This pattern is consistent with findings that certain monogeneans can adapt to or even proliferate under disturbed or nutrient-rich conditions (Abdel-Satar *et al*., 2017; Sue *et al*., 2022). The opposing distribution along the primary environmental gradient underscores niche differentiation driven by water quality, emphasizing how physicochemical factors shape parasite community structure in freshwater ecosystems. These results highlight the importance of monitoring water parameters to understand and manage parasite dynamics in aquatic habitats.

The correlation between detected heavy metals and the calculated abundance of *M. clarii* and *G. rysavyi* further illustrates species-specific responses to environmental contamination. *M. clarii* showed a strong positive association with metals such as zinc, silver, copper, bismuth, aluminum, gallium, cobalt, and manganese, suggesting a possible tolerance or preference for hosts exposed to elevated levels of these elements. Conversely, *G. rysavyi* was more closely linked to lead, cadmium, strontium, barium, and iron, indicating a different ecological niche or metal tolerance profile. These contrasting patterns align with previous studies demonstrating that parasite species vary in their sensitivity and adaptability to heavy metal pollution (Abdel-Satar *et al*., 2017; Moharam *et al*., 2024). In addition, the high abundance of *G. rysavyi* in the Al-Amlak Drain suggests that these parasites are resilient to environmental stressors, potentially serving as bioindicators of water quality. Research has shown that monogeneans can respond rapidly to changes in their environment, making them suitable candidates for monitoring ecological health (Leite *et al*., 2023).

The central positioning of both parasites in the ordination plot suggests that heavy metal contamination broadly influences their abundance, supporting their potential role as bioindicators of aquatic ecosystem health (Salgado-Maldonado *et al*., 2020). This species-specific metal association highlights the complexity of parasite-environment interactions and underscores the importance of considering multiple contaminants when assessing ecological impacts on parasite communities.

In summary, this study not only enhances our understanding of the biodiversity of ectoparasitic microfauna associated with *C. gariepinus* but also sheds light on the ecological consequences of habitat pollution and fragmentation. Future research should delve deeper into the interactions between these parasites and their hosts, especially in the context of environmental changes, to clarify their roles as bioindicators.

CONCLUSION

This research focused on the diversity of ectoparasitic microfauna found on the skin and gills of *Clarias gariepinus* in three different aquatic environments: the River Nile, a Quaternary Stream and, Al-Amlak Drain. The biodiversity and community structure of ectoparasitic microfauna on *Clarias gariepinus* are strongly influenced by environmental conditions and pollution gradients across distinct aquatic habitats in the Nile Delta. The River Nile, characterized by relatively favorable physicochemical parameters, supported the highest prevalence of *Macrogyrodactylus clarii*, while polluted sites such as Al-Amlak Drain exhibited significant parasite loads despite elevated heavy metal concentrations and hypoxic stress. Conversely, the Quaternary Stream, with lower pollution levels, harbored the most diverse parasite assemblage but lower prevalence of certain species, reflecting complex host-parasite-environment interactions. Species-specific responses to water quality and heavy metal contamination highlight the

adaptive capacity of viviparous monogeneans and their potential as bioindicators of aquatic ecosystem health. These findings underscore the critical need for integrated water quality monitoring and pollution mitigation strategies to preserve freshwater biodiversity and maintain ecological balance in the Nile Delta.

REFERENCES

ABDEL-SATAR, A. M., Ali, M.H. and Goher, M.E. 2017. Impact of heavy metals on fish parasites in the Nile River. Environmental Science and Pollution Research, 24(10), 9876–9884.

AFNOR, 2001. Eaux méthodes d'essai. In Recueil de Normes Françaises. Association Française de Normalisation. pp. 360.

AGRAWAL, N., S. RAJVANSHI, AND A. ASTHANA. 2017. Intraguild interactions between five congeneric species of *Thaparocleidus* (Monogenoidea) from the freshwater shark *Wallago attu*, Lucknow, India. Journal of Helminthology 91: 718–725. https://doi.org/10.1017/S0022149X17000049.

ALLEN, S. E., H. M. GRIMSHAY, J. A. PARKINSON, AND C. QUARMBY. 1974. Chemical Analysis of Ecological Materials. Blackwell Scientific Publications Osney, Oxforde, London, pp. 565.

CHALKOWSKI, K., C. A. LEPCZYK, AND S. ZOHDY. 2018. Parasite Ecology of Invasive Species: Conceptual Framework and New Hypotheses. Trends in Parasitology 34 (8): 655-663. https://doi.org/10.1016/j.pt.2018.05.008ز

DODGE, Y. 2008. The Concise Encyclopedia of Statistics. Springer.

EL-EMAM, D. A., S. E. ELHOSSINY, T. A. HEGAZY, AND M. A. EL-SONBATI. 2024. Assessment of Drinking Water Quality and Heavy Metal Pollution in Treatment Plants in Damietta Governorate, Egypt. Catrina: The International Journal of Environmental Sciences, 33(1):43-56. https://doi.org/10.21608/cat.2024.255996.1235.

EL-NAGGAR, A. M., M. I. MASHALAY, A. M. HAGRAS, AND H. A. ALSHAFEI. 2017. Monogenean microfauna of the Nile catfish, *Clarias gariepinus* as biomonitors of environmental degradation in aquatic ecosystems at the Nile Delta, Egypt. Journal of Environmental Science, Toxicology and Food Technology 11: 45–62. https://doi.org/10.9790/2402-1108014562

EL-NAGGAR, M. M., H. M. SERAG. 1985. The monogenean *Quadriacanthus kearni* n. sp. and a report of *Q. clariadis clariadis* Paperna, 1979 on the gills of *Clarias lazera* in Nile Delta. Journal of the Egyptian Society of Parasitology 15 :479–492.

EL-NAGGAR, M. M., H. M. SERAG. 1986 *Quadriacanthus aegypticus* n. sp., a monogenean gill parasite from the Egyptian teleost *Clarias lazera*. Systematic Parasitology 8: 129–140. https://doi.org/10.1007/BF00009869

EL-SHAER, W. AND N. H. SALLAM. 2023. Parasites Causing Respiratory Manifestations in *Mullus surmulatus* Fish from Safaga at Red Sea Governorate. Egyptian Journal of Aquatic Biology and Fisheries 27 (5): 171–184. https://doi.org/10.21608/EJABF.2023.317458.

EL SHAFEI, A., ZAHRAN, H., NASR, M., EL NOZAHI, D. 2024. 'Efficacy of the Electrocoagulation Treatment of Agricultural Drainage Water', Catrina: The International Journal of Environmental Sciences, 33(1), pp. 1-9. doi: 10.21608/cat.2024.287086.1280

ERGENS, R. 1973. Two new species of *Gyrodactylus* from *Clarias lazera* (Vermes, Trematoda, Monogenoidea), Revue de Zoologie et de Botanique Africaine, 87: 77-80.

GABR, G. A., M. F. MASOOD, E. H. RADWAN, K. H. RADWAN AND A. Z. GHOENIM. 2020. Potential Effects of Heavy Metals Bioaccumulation on Oxidative Stress Enzymes of Mediterranean clam *Ruditapes decussatus*. Catrina: The International Journal of Environmental Sciences 21 (1): 75-82. https://doi.org/10.21608/CAT.2020.2405-1.1042

GUSSEV, A. B. 1961 Aviviparous monogenetic trematode from freshwater basins of Africa, Doklady Akademy Nauka SSSR, 136: 490-493.

HAMMOND, M. E. AND R. POKORNÝ. 2020. Diversity of Tree Species in Gap Regeneration under Tropical Moist Semi-Deciduous Forest: An Example from Bia Tano Forest Reserve. Diversity 12(8): 301. https://doi.org/10.3390/d12080301

HOLMES, J. C. AND P. W. PRICE. 1986. Communities of Parasites. In: Anderson, D.J. and Kikkawa, J., Eds., Community Ecology: Patterns and Processes, Blackwell Scientific Publications, Oxford, pp. 187-213.

KARLINA, I. AND M. J. LUTHFI. 2018. Comparative Anatomy of Labyrinth and Gill of Catfish (*Clarias gariepinus*) (Burchell, 1822) and Snakehead Fish (*Channa striata*) (Bloch, 1793). Biology, Medicine, & Natural Product Chemistry 7 (2): 39-43. https://doi.org/10.14421/biomedich.2018.72.39-43

KEARN, G. C. 1994. Evolutionary expansion of the Monogenea. International Journal for Parasitology 24 (8): 1227–1271. https://doi.org/10.1016/0020-7519(94)90193-7

KRITSKY, D. C., THATCHER, V. E., & BOEGER, W. A. 1986. Neotropical monogenea. 8. revision of urocleidoides (Dactylogyridae, Ancyrocephalinae). Proceedings of the Helminthological Society of Washington, 53(1), 1-37

LEITE, L. A. R., F. F. JANUÁRIOB, L. S. PELEGRINIC, B. ANTONIASSIB, R. K. AZEVEDOD, AND V. D. ABDALLAHD. 2023. Seasonal patterns of infestation by monogenean parasites of fish and their relationship with water parameters in two rivers with different disturbance gradients in southeastern Brazil. Brazilian Journal of Biology 15 (83): e255758. https://doi.org/10.15-90/1519-698-4.255758.

LUKIN, E. I. 1976. Leeches of fresh and saline water.

In Fauna of the USSR; Nauka: Leningrad, USSR, pp. 303–351.

MOHARAM ADEL MOHAMED AFIFI, MAHMOUD RADWAN, MAHMOUD MAHROUS M. ABBAS, HOSSAM M. HWIHY, AHMED NASR ALABSSAWY, HASSAN M.M. KHALAF-ALLAH. 2024. Threat of heavy metal pollutants and parasites to freshwater fish with special reference to their risk of cancer to humans in Egypt, Aquaculture, Volume 587, 740833. https://doi.org-/10.1016/j.aquaculture.2024.740833.

OLSON, P. D. AND D. T. J. LITTLEWOOD. 2002. Phylogenetics of the Monogenea – Evidence from a medley of molecules. International Journal for Parasitology 32 (3): 233-244. https://doi.org/-10.1016/S0020-7519(01)00328-9

PAPERNA, I. 1961. Studies on monogenetic trematodes in Israel. 3. Monogenetic trematodes of the Cyprinidae and Claridae of the Lake of Galilee. Bamidgeh 13: 14–29.

APHA. 2017. Standard methods for the examination of water and wastewater (vol. 10). American public health association.

POULIN, R. 2007. Evolutionary Ecology of Parasites. 2nd Ed. Princeton University Press, Princeton: pp 332.

POULIN, R. AND C. MCDOUGALL. 2022. Fish–parasite interaction networks reveal latitudinal and taxonomic trends in the structure of host–parasite associations. Parasitology 149: 1815–1821. https://doi.org/10.1017/S0031182022000944

POULIN, R. AND S. MORAND. 2004. Parasite Biodiversity. Smithsonian Books, Washington. pp 216.

PRICE, P. W. 1980. Evolutionary Biology of Parasites. Princeton University Press. pp 237.

PRUDHOE, S. 1957 Trematoda. Exploration du Pare National de I'Upemba, Mission-G. F, de Witte, 48: 1-28.

ROHDE, K. 1979. A critical evaluation of intrinsic and extrinsic factors responsible for niche restriction in parasites. The American Naturalist 114 (5): 648-671. https://doi.org/10.1086/283514

SALEM, H. S., A. E HAGRAS, H. M. EL-BAGHDADY, AND A. M. EL-NAGGAR. 2021. Integrated Use of Nanomechanical, Histological, and Biochemical Biomarkers of *Oreochromis niloticus* as Signs of Metal Stress. Catrina: The International Journal of Environmental Sciences 23 (1): 35-43. https://doi.org/10.21608/cat.2021.196-721.

SALGADO-MALDONADO, G., J. M. CASPETA-MANDUJANO, E. F. MENDOZA-FRANCO, M. RUBIO-GODOY, A. GARCIA-VASQUEZ, N. MERCADO-SILVA, I. GUZMÁN-VALDIVIESO, AND A. M. WILFREDO. 2020. Competition from sea to mountain: Interactions and aggregation in low-diversity monogenean and endohelminth communities in twospot livebearer *Pseudoxiphophorus bimaculatus* (Teleostei: Poeciliidae) populations in a neotropical river. Ecology and Evolution 10: 9115–9131.

SOLIMAN, M. F. M., AND IBRAHIM, M. M. (2012). Monogenean community structure of Oreochromis niloticus in relation to heavy metal pollution and host reproductive cycle. Journal of the Egyptian Society of Parasitology, 42(1), 11-24.

SUE, H., K. MACKENZIE, S. C. IVES, C. C. PERT, AND C. S. JONES. 2022. *Diclidophora merlangi* (Kuhn, 1829) Krøyer, 1838 (Monogenea: Diclidophoridae) as an indicator of hydrocarbon pollution in the North Sea. Marine Pollution Bulletin, 185 (A): 114268. https://doi.org/10.1-016/j.marpolbul-.2022.114268.

SURES, B., et al. (2021). Metal accumulation in ecto- and endoparasites from the anadromous fish, the Pontic shad (Alosa immaculata). Science of the Total Environment, 778, 146192.

TER-BRAAK, C. J. 1986. Canonical correspondence analysis: A new eigenvector technique for multivariate direct gradient analysis. Ecology, 67: 1167-1179.

TER-BRAAK, C. J. 1988. CANOCO-aFORTRAN Program for canonical community ordination by partial detrended correspondence analysis, principal. Component Analysis and Redunancy Analysis (Version 2.1). Agric. Math. Group, Wageninigen, The Netherlands.

WHITTINGTON, I. D., L.A. CHISHOLM, AND K. ROHDE. 2000. The larvae of Monogenea (Platyhelminthes). Advances in Parasitology 44: 139–232. https://doi.org/10.1016/S0065308X(08)-60232-8

WILSON, J. M. AND P. LAURENT. 2002. Fish gill morphology: inside out. Journal of Experimental Zoology 293(3): 192. https://doi.org/10.10-02/jez.10124

YAMAGUTI, S. 1963. Systema helminthum IV. Monogenea and Aspidocotylea (New York, London, Sydney: Wiley Interscience.

التنوع الحيوي للكائنات الدقيقة المتوطنة على جلد وخياشيم سمكة القرموط الأفريقي *Clarias gariepinus* Burchell, 1822 في البيئات الملوثة والمجزأة

عامر أحمد نعمان، أحمد مصطفى النجار، سيد أحمد الطنطاوي، محمد إبراهيم مشالي
قسم علم الحيوان، كلية العلوم، جامعة المنصورة، مصر

الملخص العربـــــي

تتعرض النظم البيئية المائية بشكل متزايد للتهديد بسبب التلوث الناتج عن الأنشطة البشرية، مما يمكن أن يؤثر بعمق على التفاعلات بين المضيف والطفيليات والتنوع البيولوجي. إن فهم العلاقات بين الضغوط البيئية ومجتمعات الطفيليات أمر أساسي للمراقبة الفعالة وإدارة صحة المياه العذبة. لذلك تناولت هذه الدراسة التركيب المجتمعي والعوامل البيئية للميكروفونا الطفيلية الخارجية على جلد وخياشيم *Clarias gariepinus* في مناطق المختاره للدراسة عبر ثلاثة نظم بيئية في دلتا النيل: نهر النيل، مصرف الأملاك ، والمجرى الربعي. لوحظ تباين مكاني ملحوظ في المعلمات الفيزيائية والكيميائية وتركيزات المعادن الثقيلة، حيث أظهر مصرف الأملاك أعلى مستويات التلوث وأدنى مستويات الأكسجين المذاب. كانت الإصابة الطفيلية أكبر في مصرف الأملح، بينما أظهر المجري الربعي أعلى تنوع نوعي. كانت أنواع *Macrogyrodactylus* و *Gyrodactylus* أكثر انتشارًا على الجلد، في حين كانت *Piscicola geometra* مقيدة بالمواقع الملوثة. كما كشفت التحليلات المتعددة الأبعاد الاحصائيــة أن وفرة وتوزيع الطفيليات أحادية الجيل تأثرت بشكل كبير بقياسات جودة المياه المحددة وبتركيزات المعادن الثقيلة المقاسة، مع ملاحظات تاثيرالملوثات البيئية لجودة المياه علي توزيع وكثافة بين تواجد كلا من *Macrogyrodactylus* و *Gyrodactylus* كطفيليات التي تم دراستها علي جسم وخياشيم *Clarias gariepinus*. كما تبرز هذه النتائج فائدة الطفيليات أحادية الجيل بناء علي مدي ارتباطها بالملوثات وخصوصا المعادن الثقيلة انه يمكن استحدامها كمؤشرات حيوية حساسة لتقييم صحة النظم البيئية المائية العذبة وتأثيرات التلوث.